

---

# Object Localization and Motion Transfer learning with Capsules

---

**Weitang Liu**

Department of Electrical and Computer Engineering  
University of California, Davis  
Davis, CA 95616 USA  
wetliu@ucdavis.edu

**Emad Barsoum**

Microsoft  
One Microsoft Way, WA 98052 USA  
ebarsoom@microsoft.com

**John D. Owens**

Department of Electrical and Computer Engineering  
University of California, Davis  
Davis, CA 95616 USA  
jowens@ece.ucdavis.edu

## Abstract

Inspired by CapsNet’s routing-by-agreement mechanism, with its ability to learn object properties, and by center-of-mass calculations from physics, we propose a CapsNet architecture with object coordinate atoms and an LSTM network for evaluation. The first is based on CapsNet but uses a new routing algorithm to find the objects’ approximate positions in the image coordinate system, and the second is a parameterized affine transformation network that can predict future positions from past positions by learning the translation transformation from 2D object coordinates generated from the first network. We demonstrate the learned translation transformation is transferable to another dataset without the need to train the transformation network again. Only the CapsNet needs training on the new dataset. As a result, our work shows that object recognition and motion prediction can be separated, and that motion prediction can be transferred to another dataset with different object types.

## 1 Introduction

Humans in their early years learn the motion of objects intuitively. They are able to not only learn to recognize objects, but also locate objects and predict their motion. They gradually learn to summarize the motion rules that apply to objects they have never seen before. In kinematics problems, such as predicting the trajectory of a ball, objects are often simplified as point masses [20], which serve as the input to equations of motion. This demonstrates coordinates are one of the key concepts that unify solutions with different objects in kinematic problems.

In physical simulation frameworks, the physics of the environment is modeled by predefined rules. These rules determine how objects move in the scene, and then the physics system generates affine transformation matrices that the graphics system consumes to render objects in the proper positions on the screen. Our idea is to reverse this process. As a powerful function approximation tool, the neural network can determine the affine transformation matrices for each object, frame-by-frame, through the learned physics rules of the underlying physical environment. Such a network should be able to model the rules that generate transformation matrices not only for objects it has seen before, but also for unknown objects in the same environment. This is similar to the case of predicting the trajectory of a baseball through learning the trajectory of throwing other objects. In this paper, we only consider the translational transformation.

As a variant of a convolution neural network (CNN), CapsNet [14] has been recently proposed to better describe objects' properties with vector-based activation and specially designed routing algorithms. The capsules encode the pose information that is more general than a scalar value representing the presence of an object as in CNN. The routing algorithm makes this pose information useful to form object hierarchies. Low-level capsules activate and vote by pose agreement to determine which high-level capsules will be activated, creating a part-whole relationship between the low-level capsule and the high-level capsules. As a result, each dimension of a capsule represents some properties of the object, such as stroke thickness of digits in the MNIST dataset. Moreover, by manually changing the value of each dimension in the digit capsules, Sabour et al. [14] showed that these properties can be controlled and visualized through reconstruction layers. As low-level capsules that share similar poses are routed to form high-level capsules, coordinates of high-level capsules' centers can be derived by averaging the activated low-level capsules. These high-level coordinates will be able to approximate the position of objects' centers.

Our contributions are as follows. We propose an algorithm to derive the approximate coordinates of object centers in the image coordinate system through CapsNet. We also propose a parameterized transformation network to learn the translation rules based on these coordinates. These translation rules can generate the proper transformation matrices for specific objects. By pre-training two CapsNets for the moving Fashion MNIST and moving MNIST datasets generated by Szeto et al. [18], we demonstrate that a parameterized transformation network trained on the moving MNIST dataset can automatically transfer the translation knowledge to the moving Fashion MNIST.

Our paper is organized as follows. Section 2 lists the related work. Section 3.1 introduces the algorithm which derives the coordinates through CapsNet. Section 3.2 proposes simple parameterized transformation network for learning the translational transformation matrix. Section 4.2 demonstrates through experiments that our CapsNet is able to derive coordinates. Section 4.4 shows that the learned translational knowledge is transferable between different datasets, as long as the CapsNet learns to recognize the objects. Section 4.5 discusses the limitations of our proposed models, and discusses some drawbacks .

## 2 Related Work

Sabour et al. [14] recently proposed CapsNet with a dynamic routing algorithm. By replacing the max-pooling layer with a routing-by-agreement algorithm, CapsNet ensures that lower-level capsules send their information to higher-level capsules properly. By explicitly concatenating the coordinates of the lower-level capsules and then routing-by-agreement, our proposed algorithm can derive the objects' center of mass at the higher-level capsules from the lower-level capsules. Recently, Hinton et al. [6] proposed the EM (expectation-maximization) routing algorithm with a coordinate addition. Our algorithm is inspired by the coordinate addition, but we explicitly utilize these coordinate information in the reconstruction layers. We suggest that the coordinates are useful not only in routing as Hinton et al. mentioned, but also in deriving the coordinates of high-level capsules as a fundamental property in learning translational motions.

Many algorithms identify the positions of objects. Supervised learning algorithms [10, 12, 13] require bounding boxes and classes as inputs to train the recognition networks. Weakly supervised methods [15] usually only require the objects' classes as inputs to train the network. However, the objects' positions are derived from active spots represented by the gradients of the last few convolution layers. Our method requires the input image, classification ground truth, and coordinate addition in the routing process. By manually tweaking the capsules' coordinate atoms, the reconstruction layers will generate images with the object appear in the modified position. This shows the coordinates our method finds are controllable properties of the objects.

Srivastava et al. [17] has proposed an LSTM model for predicting future frames on the moving MNIST dataset with two digits and on the UCF-101 dataset, which is more complicated than our moving MNIST dataset. The future frame predictions of the work are purely unsupervised. Our proposed method focuses on the fact that CapsNet, once it is well-trained, is able to reason out object properties, such as the coordinates of objects' centers, that are potentially useful for generalization and transfer learning.

Recently, unsupervised learning for video prediction [3, 19] has become a popular topic. Many methods [11, 7, 8] predict frames through generated adversarial networks [5]. Newer frameworks [1, 16]

are able to generate frames with stochastic futures. Frame prediction through affine transformation [2] is also a common topic today. Compared with these sophisticated models, our parameterized network focuses on what knowledge is transferable between different datasets. We believe sophisticated affine transformation models can be easily merged with our work.

In this paper, we show that object appearance and its motion can be separated, and the motion part can be transferred to another dataset. The separation of the objects and the motion rules is supported by the two-stream [4] hypothesis in neural science. The ventral stream is responsible for the object recognition, while the dorsal stream is responsible for the spatial aspects of vision. In our setting, the CapsNet works similarly as a ventral stream, while the parameterized affine transformation network works as a dorsal stream.

### 3 Model Architecture

#### 3.1 CapsNet with coordinate atoms

We adopt a similar architecture to CapsNet [14]. After the primary-caps layer, the capsules are multiplied by the transformation matrices. We then concatenate two additional atoms to each of the capsules, according to the capsules’ relative position in the feature map. Thus, the capsules are 18 dimensions instead of 16. These two atoms are normalized from 0 to 1. This setting is similar to the coordinate addition Hinton et al. performed in the EM-Routing version of CapsNet [6]. For example, if the feature map after the primary-cap layer has spatial dimensions of 7x7, and the calculated receptive field is 9x9, then the capsule representing the top-left corner has coordinate values of  $[x, y] = [4/64, 4/64]$ , where 64 is the original image size and 4 is half of 9. The routing algorithm also considers these two coordinate atoms as well. During the routing, 16 atoms, excluding the two coordinate atoms, are passed to the activation function. To simplify the routing process, we concatenate the coordinate atoms and the other 16 atoms only when the logits are updated and output capsules are returned.

The routing probabilities of the low-level capsules,  $c_i$ , are utilized to determine the coordinates of the high-level capsules through a weighted average

$$coordinates_j^l = \frac{\sum_i^n c_{i,j} \cdot coordinates_{j|i}^{l-1}}{\sum_i^n c_{i,j}} \tag{1}$$

where the  $l$  denotes the digit-cap layer, and  $l - 1$  denotes the primary-cap layer. The  $n$  denotes the number of channels, and  $j$  denotes the  $j$ th output capsule. This equation is simply taking the object coordinates from each lower-level capsule, and weighting them by the coupling coefficient, which predicts how closely related the lower-level and higher-level capsules are. The *coordinates* represents a vector of the coordinates.

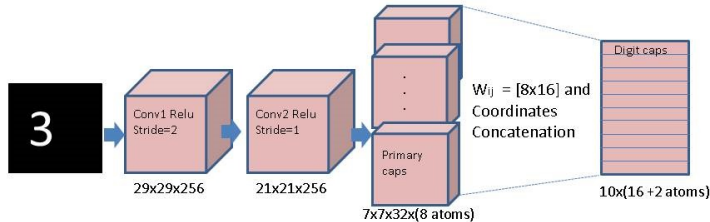


Figure 1: Modified CapsNet layers. Two convolution layers with different strides extract features before the primary-cap layer. In the primary-cap layer, each capsule after being multiplied by the weight matrix is then concatenated with the coordinate atoms before routing.

The new architecture for the CapsNet is summarized in Figure 1, and the reconstruction layers are shown in Figure 2. The figures shown here are in HWC format, the input image is the number 3, and 10 is the number of outputs representing the 10 digits. The CapsNet has two convolution layers, each of which has 256 9x9 filters. The stride of the first convolution layer is 2, while the stride of

the second convolution layer is 1. A primary-caps layer with strides equal to 2 has 32 9x9 kernels with 8 atoms. Each capsule with 8 atoms is then multiplied by weight matrices  $W_{ij}$  to get 16 atoms. Each capsule is then concatenated with two coordinate atoms before routing. The total number of atoms in a capsule is then 18, thus the size of the digit-caps layer (after routing) is 10x18. We observe slightly better results if the reconstruction layers are convolution-transpose layers instead of fully connected layers. Our reconstruction layers are four convolution layers with 3x3, 3x3, 4x4, 8x8 kernels. Both the classification loss and the reconstruction loss are the same as in CapsNet [14]. The routing algorithm with the coordinates is described by algorithm 1.

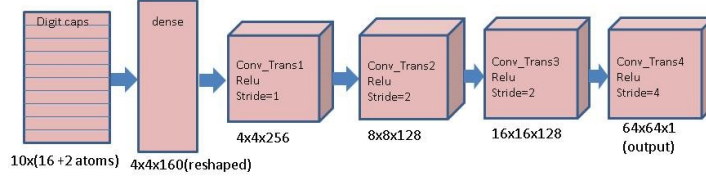


Figure 2: Modified reconstruction layers. The digit-cap layer is flattened and fed as an input to a fully-connected layer. Convolution transpose layers are used. The output of the last convolution layer is a 64x64 image.

---

**Algorithm 1:** Routing with coordinates from primary-caps to digit-caps.

---

**Result:** Digit-caps with coordinates

- 1 for capsules  $i$  in primary-caps layer and  $j$  in digit-caps layer: initialize logits  $b_{ij}$  ;
  - 2 for all capsules  $j$  in digit-caps:  $u_j^{new} = concatenate(coords_{j|i}, \hat{u}_{j|i})$  ;
  - 3 **for**  $r$  iterations **do**
  - 4     for all capsules  $i$  in primary-caps:  $c_i = softmax(b_i)$ ;
  - 5     for all capsules  $j$  in digit-caps:  $s_j = \sum_i c_{ij} \hat{u}_{j|i}$ ;
  - 6     for all capsules  $j$  in digit-caps:  $v_j = squash(s_j)$ ;
  - 7     for all capsules  $j$  in digit-caps:  $o_j = \frac{\sum_i c_{ij} coords_{j|i}}{\sum_i c_{ij}}$  ;
  - 8     for all capsules  $j$  in digit-caps:  $v_j^{new} = concatenate(o_j, v_j)$  ;
  - 9     for all capsules  $i$  in primary-caps and for all capsules  $j$  in digit-caps:  $b_{ij} = b_{ij} + \hat{u}_{j|i}^{new} \cdot v_j^{new}$
  - 10 **end**
- 

### 3.2 Parameterized affine transformation layer

We add a simple affine transformation layer to parameterize the affine transformation learned from objects. It consists of a Conv-LSTM layer and a convolution layer. After the digit-caps layer, the two coordinate atoms are separated from the capsules; these two coordinate atoms and the LSTM state are then concatenated and fed as inputs to the conv-LSTM. Since only the coordinates are considered, this transformation layer is a demonstration of learning the translational motions as “the objects will move in the same speed and direction, and bounce back if they get too close to the canvas boundary.” Since this layer remembers the motions according to the digits’ own coordinates, they will not be able to model complicated inter-object relationships. In computer graphics, the motions will be more complicated, but they should be easily parameterized through layers with considerations of other capsules’ representations and the image feature maps.

More specifically, the state input of the conv-LSTM is two stacked tensors each with 32 channels, while the coordinate atoms are only 2 channels. The state input splits into two 32-channel tensors,  $h$  and  $c$ ;  $h$  and coordinates will be concatenated together as an input to the conv-LSTM. After the  $h_{new}$  is derived, which should have 32 channels, it will then be fed into another convolution layer which outputs a tensor with 6 channels. These 6 channels are reshaped to 3 by 2 matrices as affine transformation matrices, which will multiply the coordinates. This setting is similar to Lin et al. [9]. The transformation matrix proposed here is more complicated than the translation transformation requires. Thus, the output of the last convolution layer can be only 2 channels for translation instead of 6. The conv-LSTM layer and the convolution layer use 1x1 kernels to ensure weight sharing

between different digit capsules. We split the samples in the time axis and feed them, frame by frame, into the CapsNet, affine transformation layer, and reconstruction layers. The first 10 frames are used to warm up the state representations, and the loss is accumulated after the warm up frames.

The loss function we use here can be either only a reconstruction loss or the coordinate atoms loss, which is defined as:

$$loss_{coords} = \frac{1}{m} \sum_i^m (coords_i^{re} - coords_i^{ge})^2 \quad (2)$$

where  $m$  is the batch size,  $coords^{re}$  is the current coordinate atoms derived by real images, and  $coords^{ge}$  is the current coordinates calculated by multiplying the affine transformation matrices with the previous coordinates. In a preliminary experiment, we found that training with this coordinates' L2 loss is slow because both the capsules of the future ground truth frames and the predicted frames are required, but the improvement is minor. Thus, in this paper, we will keep the reconstruction loss only. In another preliminary experiment, we replace the conv-LSTM layer with a convolution layer. Compared with the loss of a model with conv-LSTM layer, the training loss of a model with convolution layer is generally higher. We simply stick with conv-LSTM.

The architecture of the affine transformation layer is summarized in Figure 3.

Finally, in order to constrain the coordinates to range 0 to 1 after the affine transformation, we add a spill loss, which is defined as

$$loss_{spill} = \frac{1}{m} \sum_{i,j,k} \max(0, coords_{i,j,k} - 1.) + \max(0, -coords_{i,j,k}) \quad (3)$$

where  $m$  is the batch size,  $j$  is the number of in channels, and  $k$  is the number of capsules' dimension.

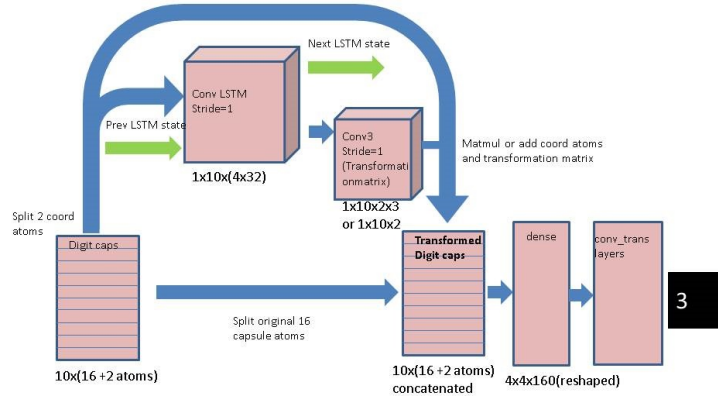


Figure 3: Illustration of the affine transformation layer, which transforms the coordinates by affine transformation matrices. It consists of a Conv-LSTM layer and a convolution layer. Transformation matrices are parameterized by the LSTM state and coordinate atoms. The output of the Conv3 layer can either be 6 (affine transformation matrix) or 2 (only translation), because only translation is considered in our paper.

## 4 Experiments

### 4.1 Datasets

These models are tested using the moving MNIST dataset and the moving Fashion MNIST dataset generated through Szeto et al. [18], which can set different moving speeds of the digits. The speed of each sample is a random variable ranging from 1 to 9. The samples have translation motion only. The sequence length is 20, which is the number of frames per sample (time axis). In order to fulfill the requirement of point mass, the images of both the MNIST and Fashion MNIST dataset are resized to  $16 \times 16$ . Each sample contains only one handwritten digit, generated by placing a  $16 \times 16$  MNIST sample on a  $64 \times 64$  canvas. We generate two training sets and two test sets for moving MNIST and moving Fashion MNIST; each training set has 30,000 samples and each test set has 1,000 samples.

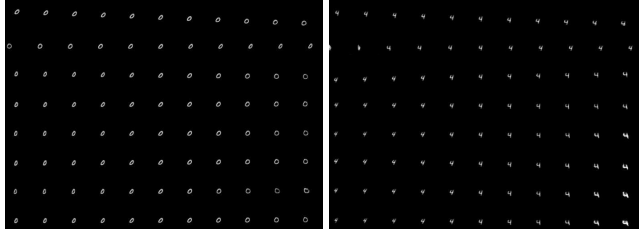


Figure 4: Dimension perturbations of the moving MNIST dataset. Each row is generated by perturbing one dimension’s value from -0.25 to 0.25 with step 0.05. Only 8 of the 18 dimensions are shown here. The first two rows are perturbations of the coordinate atoms.

Frames for digit 3										
x atom	0.11	0.20	0.34	0.48	0.64	0.78	0.87	0.90	0.89	0.86
y atom	0.14	0.14	0.13	0.11	0.10	0.10	0.10	0.10	0.10	0.10
Frames for digit 6										
x atom	0.45	0.54	0.63	0.70	0.77	0.83	0.87	0.89	0.88	0.85
y atom	0.19	0.25	0.31	0.38	0.47	0.56	0.65	0.71	0.76	0.81

Figure 5: Coordinate atoms of 10 consecutive ground truth frames for two digits. The coordinate atoms are normalized from 0 to 1. 0 represents top ( $x$  atom) or left ( $y$  atom) of the canvas, while 1 represents bottom ( $x$  atom) or right ( $y$  atom) of the canvas.

## 4.2 CapsNet as a position identifier

The first experiment tests if CapsNet is able to extract the coordinates within the image coordinate system. Thus, only images are considered as samples. We randomly pick and shuffle 15 frames out of the 20 frames in the time axis. The result is the number of samples in this experiment:  $15 \times 30,000 = 450,000$ . The reconstruction balanced factor is 0.005. The number of routing iterations is 5 instead of 3.

We build our model according to the architecture in subsection 3.1. The batch size is 100 with 60 training epochs. Figure 4 is a dimension perturbation of the first 8 dimensions of a digit capsule. This figure shows the change of the coordinate atoms (first two rows), resulting in a change of the digits’ positions. This indicates that CapsNet with coordinate atoms can successfully capture the object coordinates, and the reconstruction layers can generate the images according to the values of the coordinate atoms. The first coordinate atom (first row) in Figure 4 represents the vertical axis, and the second coordinate atom (second row) represents the horizontal axis; they match our coordinate addition scheme in subsection 3.1.

Figure 5 shows two examples of a randomly picked sequence of ground truth frames and their correspond coordinate atoms. In the table,  $x$  is the vertical axis and  $y$  is the horizontal axis. They are normalized from 0 to 1, where the 0 for the  $x$  atom is the top of the canvas and 0 for the  $y$  atom is the left of the canvas. As an example, the  $x$  atom is 0.11 and the  $y$  atom is 0.14 for the first frame of digit 3. These coordinates indicate the digit should be at the top left corner of the canvas. All the  $x, y$  coordinates correspond to the digits’ positions in the sense of the above explanation.

## 4.3 Parameterized translational transformation

We load and fix the pre-trained model as in subsection 4.2, and then add the affine transformation layer as in subsection 3.2. This layer is only for training the coordinate atoms. In this experiment, we will feed the first 10 ground truth frames of each sample to the network to warm up the LSTM state, and the network will predict the next 10 frames by self-feeding the capsules to the network instead of the reconstructed images. After the first 10 ground truth frames, the 16 atoms of each capsule,



(a) Ground truth frames for digit 6 and 2



(b) Generated frames for digits 6 and 2 with affine transformations

Figure 6: Two examples of digits' ground truth frames and reconstruction frames after transformation. The reconstruction frames are generated in a "self-feed" manner.



(a) Ground truth frames for two classes Fashion MNIST



(b) Generated images for two classes Fashion MNIST

Figure 7: Two examples of Fashion MNIST ground truth frames and reconstruction frames after transformation. The transformation matrices are not trained on the moving Fashion MNIST dataset, but a pre-trained CapsNet for the Fashion MNIST is required for image reconstruction and coordinates.

excluding the two coordinate atoms, will be fixed for prediction. These 16 atoms will be concatenated with the updated coordinate atoms as an input to the reconstruction layers. Only an L2 reconstruction loss is applied to the difference between the 10 predicted frames and the last 10 ground truth frames. The output channel of Conv3 is 2 instead of 6, because only translation is considered. The batch size is 25 and the training set contains 30,000 samples.

Two prediction results after 50 epochs are shown in Figures 6(a) and 6(b). Only the last 10 frames are shown.

#### 4.4 Transfer learning from MNIST dataset to Fashion MNIST dataset

The models are also tested in a transfer learning scenario. The moving MNIST and moving Fashion MNIST data sets are generated in the same setting. The affine transformation layer is pre-trained on the moving MNIST dataset, and the CapsNet model is pre-trained on the moving Fashion MNIST dataset as in subsection 4.2. We want to test if the learned modeling of the translation knowledge is transferable when the CapsNet model knows the objects (Fashion MNIST) well. The results are in 7(a) and 7(b). Even though the generated images are not perfect, these two examples clearly show that the objects' translational knowledge is transferable. More discussion of the difference between ground truth and the generated frames around the boundary is in subsection 4.5.

#### 4.5 Discussion of experiments and failure case studies

We will summarize our models by pointing out some of our models' drawbacks through examples of failure cases. We notice that our model fails to predict future frames that look exactly like the ground-truth frames. One known problem is when CapsNet and its reconstruction layers fail to recognize the coordinates. For example, the CapsNet model fails to generate the image according to the perturbation of the two coordinate atoms in a digit capsule, as shown in Figure 8(a). In this test case, the reconstruction layers wrongly associate the second coordinate with the vertical axis. The coordinate atoms it finds are [0.25 0.71], which roughly correspond to its position as in Figure 8(b). We conjecture that a better reconstruction layer and more training examples would help the CapsNet capture the coordinates.

Another failure case is when the objects get near the canvas boundary. Because of the relative size of the objects (16x16) compared to the size of the canvas (64x64), the shape of the objects cannot be ignored and the objects cannot simply be replaced by the center coordinates. When

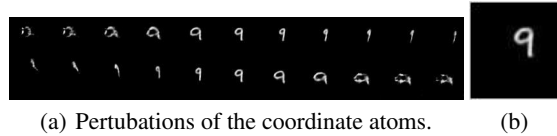


Figure 8: Failure case of dimension perturbation of the coordinate atoms.

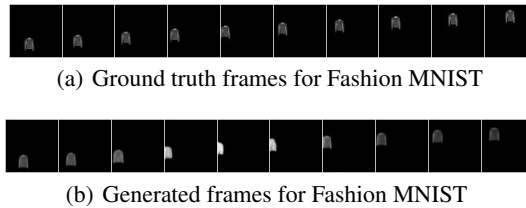


Figure 9: Failure case of an object boundary near the canvas boundary. Compared with the ground truth frames, the reconstruction frames show the coat is getting too close to the boundary before it bounds back.

the object boundary is near the canvas boundary, the generated frames are often different from ground-truth frames. This difference suggests that in this relative scale (16x16 objects in a 64x64 canvas), generating future frames using only the coordinate atoms is often not enough when the objects get close to the boundary. In this case, the shapes or the bounding boxes of the objects must be considered. Figure 9 is an example of this failure. In the transfer learning scenario, because the translation transformation is learned from the digits' coordinates, the network fails to realize the coat has a larger bounding box than the digits have, and thus fails to generate frames that look like the ground truth frames.

Finally, we notice that the CapsNet and its reconstruction layers often find the atoms that represent mixed properties. Usually, finding the atoms with mixed properties, such as mixture of stroke thickness and skew, don't matter for frame prediction. However, the two rows in Figure 8(a) indicate the second coordinate atom captures the information from both the vertical and the horizontal axis. This mixture of the properties leads to a failure of generating the correct future frames.

## 5 Discussion and future work

In this paper, we showed a novel use of CapsNet to both predict a translation transform for a moving object, and transfer such knowledge to an unknown object without retraining. One of the main characteristics of our CapsNet is to derive object spatial information. We believe this approach is promising, but we note some limitations, such as the inability of generating a proper orthogonal representation when the atom coordinate represents stroke thickness in addition to the translation coordinate.

In future work, we plan to focus on improving this CapsNet architecture in order to generate a more robust representation of a translation transform. Furthermore, object motion includes not only translation, but rotation as well. The challenge of supporting rotation is that it cannot be derived by the center of gravity only, and thus this is a challenge we hope to investigate in future work as well.

## References

- [1] Mohammad Babaeizadeh, Chelsea Finn, Dumitru Erhan, Roy H. Campbell, and Sergey Levine. Stochastic variational video prediction. In *International Conference on Learning Representations*, 2018.
- [2] Baoyang Chen, Wenmin Wang, and Jinzhuo Wang. Video imagination from a single image with transformation generation. In *Proceedings of the Thematic Workshops of ACM Multimedia 2017*, pages 358–366. ACM, 2017.

- [3] Chelsea Finn, Ian Goodfellow, and Sergey Levine. Unsupervised learning for physical interaction through video prediction. In *Advances in Neural Information Processing Systems*, pages 64–72, 2016.
- [4] Melvyn A Goodale and A David Milner. Separate visual pathways for perception and action. *Trends in Neurosciences*, 15(1):20–25, 1992.
- [5] Ian Goodfellow, Jean Pouget-Abadie, Mehdi Mirza, Bing Xu, David Warde-Farley, Sherjil Ozair, Aaron Courville, and Yoshua Bengio. Generative adversarial nets. In *Advances in Neural Information Processing Systems*, pages 2672–2680, 2014.
- [6] Geoffrey Hinton, Sara Sabour, and Nicholas Frosst. Matrix capsules with EM routing. 2018.
- [7] Alex X Lee, Richard Zhang, Frederik Ebert, Pieter Abbeel, Chelsea Finn, and Sergey Levine. Stochastic adversarial video prediction. *arXiv preprint arXiv:1804.01523*, 2018.
- [8] Xiaodan Liang, Lisa Lee, Wei Dai, and Eric P. Xing. Dual motion gan for future-flow embedded video prediction. pages 1762–1770, 10 2017.
- [9] Tsung-Yu Lin, Aruni RoyChowdhury, and Subhransu Maji. Bilinear CNN models for fine-grained visual recognition. In *Proceedings of the IEEE International Conference on Computer Vision*, pages 1449–1457, 2015.
- [10] Wei Liu, Dragomir Anguelov, Dumitru Erhan, Christian Szegedy, Scott Reed, Cheng-Yang Fu, and Alexander C Berg. Ssd: Single shot multibox detector. In *European Conference on Computer Vision*, pages 21–37. Springer, 2016.
- [11] Michael Mathieu, Camille Couprie, and Yann LeCun. Deep multi-scale video prediction beyond mean square error. *arXiv preprint arXiv:1511.05440*, 2015.
- [12] Joseph Redmon, Santosh Divvala, Ross Girshick, and Ali Farhadi. You only look once: Unified, real-time object detection. In *Proceedings of the IEEE Conference on Computer Vision and Pattern Recognition*, pages 779–788, 2016.
- [13] Shaoqing Ren, Kaiming He, Ross Girshick, and Jian Sun. Faster R-CNN: Towards real-time object detection with region proposal networks. In *Advances in Neural Information Processing Systems*, pages 91–99, 2015.
- [14] Sara Sabour, Nicholas Frosst, and Geoffrey E Hinton. Dynamic routing between capsules. In *Advances in Neural Information Processing Systems*, pages 3859–3869, 2017.
- [15] Ramprasaath R Selvaraju, Michael Cogswell, Abhishek Das, Ramakrishna Vedantam, Devi Parikh, and Dhruv Batra. Grad-cam: Visual explanations from deep networks via gradient-based localization. 2016.
- [16] Rui Shu, James Brofos, Frank Zhang, Hung Hai Bui, Mohammad Ghavamzadeh, and Mykel Kochenderfer. Stochastic video prediction with conditional density estimation. 2016.
- [17] Nitish Srivastava, Elman Mansimov, and Ruslan Salakhudinov. Unsupervised learning of video representations using LSTMs. In *International Conference on Machine Learning*, pages 843–852, 2015.
- [18] Ryan Szeto, Simon Stent, German Ros, and Jason J. Corso. A dataset to evaluate the representations learned by video prediction models. In *International Conference on Learning Representations (Workshop Track)*, April 2018.
- [19] Vedran Vukotić, Silvia-Laura Pintea, Christian Raymond, Guillaume Gravier, and Jan C van Gemert. One-step time-dependent future video frame prediction with a convolutional encoder-decoder neural network. In *International Conference on Image Analysis and Processing*, pages 140–151. Springer, 2017.
- [20] E.T. Whittaker and W. McCrae. *A Treatise on the Analytical Dynamics of Particles and Rigid Bodies*. Cambridge Mathematical Library. Cambridge University Press, 1988.